



RADIATION ABSORPTION AND DUFOUR EFFECTS TO MHD FLOW IN VERTICAL SURFACE

Damala Chenna Kesavaiah¹ & P V Satyanarayana²

¹Department of H & BS, Visvesvaraya College of Engineering & Technology, MP Patelguda, Ibrahimpatnam, R.R. Dist -501510, Hyderabad AP, India.

²Fluid Dynamics Division, School of Advanced Sciences, VIT University, Vellore - 632 014, TN, India.

Abstract

The present paper is the effects of radiation absorption, chemical reactions and Diffusion thermo (Dufour effect) effects to MHD flow of an electrically conducting, incompressible, viscous fluid past an impulsively moving isothermal vertical plate through porous medium in the presence of uniform suction. A flow of this type represents a new class of boundary layer flow at a surface of finite length. The equations governing the flow field are solved by analytical method. The velocity, temperature, concentration and skin friction have been evaluated for variation in the different governing parameters.

Keywords: Chemical reaction, Heat generation, Heat and Mass flux and Radiation absorption.

1. Introduction

Some of the typical application of such study is polymer sheet extrusion from a dye, glass fiber and paper production, drawing of plastic films etc. A great deal of literature is available on the two-dimensional visco-elastic boundary layer flow over a stretching surface where the velocity of the stretching surface is assumed linearly proportional to the distance from a fixed origin. Flow and heat transfer study over moving smooth surfaces are of immense effect in many technological processes, such as the aerodynamic extrusion of plastic sheet, rolling, purification of molten metal from non-metallic inclusion by applying magnetic field and extrusion in manufacturing processes. In continuous casting, consists of pouring molten metal into a short vertical metal die or mould, which is open at both ends, colling the melt rapidly and withdrawing the solidified product in a continuous length from the bottom of the mould at a rate consistent with that of pouring, the casting solidified before leaving the mould. The mould is cooled by circulating water around it. The process is used for producing blooms, billets and slabs for rolling structural shaped, it is mainly employed for copper, brass, bronze, aluminium and also increasingly with cast iron and steel.

Heat source and chemical reaction effects are crucial in controlling the heat and mass transfer. The present paper attempts to investigate the influence of chemical reaction and the combined effects of internal heat generation and the convective boundary condition on the MHD heat and mass transfer flow. To the best of the authors' knowledge, so far no one has considered the combined effect of chemical reaction and heat source along with convective surface boundary condition on MHD flow and the heat and mass transfer over a moving vertical plate. This fact motivated us to propose the similar study. We extend the recent work of (Makinde, 2010; Olanrewaju et al. 2012; Gangadhar et al., 2012) to expose the effect of chemical reaction on MHD heat and mass transfer over a moving vertical plate in presence of heat source along with convective surface boundary condition. The coupled nonlinear partial differential equations governing the flow, heat and mass transfer have been reduced to a set of coupled nonlinear ordinary differential equations by using similarity transformation. (Chenna Kesavaiah and Satyanarayana, 2013) MHD and Diffusion thermo effects on flow accelerated vertical plate with chemical reaction.

The study of heat generation or absorption in moving fluid is important in problems dealing with dissociating fluids. Possible heat generation effect may alter the temperature distribution; consequently, the particle deposition rate in nuclear reactors, electronic chips and semi conductor wafers. (Rahman et al., 2009) studied thermo - micropolar fluid flow along a vertical permeable plate with uniform surface heat flux in the presence of heat generation. (Ibrahim , 2009) found the analytic solution of MHD mixed convection heat and mass transfer over an isothermal, inclined permeable stretching plate immersed in a uniform porous medium in the presence of chemical reaction, internal heating, Dufour effect and Hall effects. (Pal and Chatterjee, 2010) studied heat and mass transfer in MHD non-Darcian flow of a micropolar fluid over a stretching sheet embedded in a porous media with non-uniform heat source and thermal radiation. (Chambree and Young, 1958) have analyzed a first order chemical reaction in the neighbourhood of a stationary horizontal plate. (Das et al, 1994) have studied the effect of homogeneous first order chemical reaction on the flow past an impulsively started infinite vertical plate with uniform heat flux and mass transfer. Again, mass transfer effects on moving isothermal vertical plate in the presence of chemical reaction studied by (Das et al, 1998). The dimensionless governing equations were solved by the usual Laplace-trans form technique and the solutions are valid only at lower time level. Radiation and chemical reaction effects on isothermal vertical oscillating plate with variable mass diffusion have been studied by (Manivannan et al, 2009; Rout et .al., 2013) MHD Heat and mass transfer of chemical reaction fluid flow over a moving vertical plate in presence of heat source with convective surface boundary condition.

The aim of the present works we contemplate to study the radiation absorption, chemical reactions and Diffusion thermo (Dufour effect) to MHD flow of an electrically conducting, incompressible, viscous fluid past an impulsively moving isothermal vertical plate through porous medium in the presence of uniform suction, uniform heat and mass flux.

2. Formulation of the Problem

We consider the steady, two-dimensional laminar, incompressible flow of a chemically reacting, viscous fluid on a continuously moving vertical surface in the presence of a uniform magnetic field, radiation absorption with heat generation, uniform heat and mass flux effects issuing a slot and moving with uniform velocity in a fluid at rest. Let the x-axis be taken along the direction of motion of the surface in the upward direction and y-axis is normal to the surface. The temperature and concentration levels near the surface are raised uniformly. The induced magnetic field, viscous dissipation is assumed to be neglected. Now, under the usual Boussinesq's approximation, the flow field is governed by the following equations.

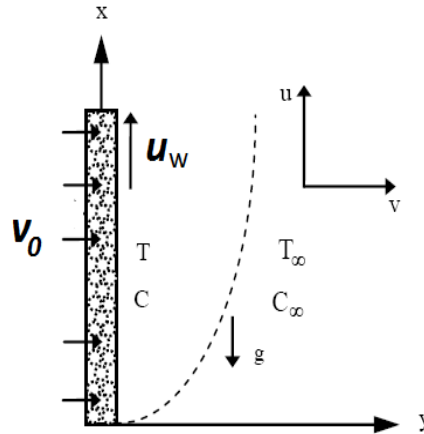


Figure (a): Flow configuration and coordinate system

Continuity equation

$$u \frac{\partial u}{\partial x} + v \frac{\partial v}{\partial y} = 0 \quad (1)$$

Momentum equation

$$u \frac{\partial u}{\partial x} + v \frac{\partial u}{\partial y} = g\beta(T' - T'_\infty) + g\beta^*(C' - C'_\infty) + \nu \frac{\partial^2 u}{\partial y^2} - \frac{\sigma B_0^2}{\rho} u - \frac{\nu}{K_p} u \quad (2)$$

Energy equation

$$\rho C_p \left(u \frac{\partial T'}{\partial x} + v \frac{\partial T'}{\partial y} \right) = k \frac{\partial^2 T'}{\partial y^2} - Q_0 (T' - T'_\infty) + Q_l' (C' - C'_\infty) + \frac{D_M K_T}{c_s c_p} \frac{\partial^2 C'}{\partial y^2} \quad (3)$$

$$u \frac{\partial C'}{\partial x} + v \frac{\partial C'}{\partial y} = D \frac{\partial^2 C'}{\partial y^2} - Kr'(C' - C'_\infty) \quad (4)$$

The relevant boundary conditions are

$$u = u_w, v = -v_0 = \text{const} < 0$$

$$\frac{\partial T'}{\partial y} = -\frac{q}{k}, \frac{\partial C'}{\partial y} = -\frac{j''}{D} \quad \text{at } y = 0 \quad (5)$$

$$u \rightarrow 0, T' \rightarrow T'_\infty, C' \rightarrow C'_\infty \quad \text{as } y \rightarrow \infty$$

In order to write the governing equations and the boundary conditions the following non dimensional quantities are introduced.

$$u = \frac{u}{u_w}, Y = \frac{y v_0}{\nu}, T = \frac{T' - T'_\infty}{\left(\frac{qv}{kv_0} \right)}, C = \frac{C' - C'_\infty}{\left(\frac{j''v}{kv_0} \right)}, k = \frac{K_p v_0^2}{\nu^2}, M = \frac{\sigma B_0^2 \nu}{\rho v_0^2}, Q = \frac{\nu Q_0}{\rho C_p v_0^2}, Sc = \frac{\nu}{D_M} \quad (6)$$

$$Pr = \frac{\mu C_p}{k}, Kr = \frac{Kr'v}{v_0^2}, Q_l = \frac{Q_l' j''v}{qv_0^2 \rho C_p}, Gr = \frac{\nu g \beta \left(\frac{qv}{kv_0} \right)}{u_w v_0^2}, Gc = \frac{\nu g \beta^* \left(\frac{j''v}{kv_0} \right)}{u_w v_0^2}, Du = \frac{D_M K_T j''}{c_s c_p \nu q \rho C_p}$$

Where u, v are the velocity along the x, y -axis, is constant obtained after integration conservation of mass in pre-non dimensional form not mentioned, ν is the kinematic viscosity, g is the acceleration due to gravity, T' is the temperature of the fluid, is the coefficient of volume expansion, C_p is the specific heat at constant pressure, is a constant, σ is the Stefan-Boltzmann constant, T'_w exceeds the free steam temperature T'_∞ , C' is the species concentration, is the wall temperature, C'_w is the concentration at the plate, T'_∞ is the free steam temperature far away from the plate, C'_∞ is the free steam concentration in fluid far away from the plate, Pr is the Prandtl number, Gr is the Grashoff number, k is the thermal conductivity of the fluid, B_0 is uniform magnetic field strength, M is the magnetic field parameter which is the ratio of magnetic force to the inertial force. It is a measure of the effect of flow on the magnetic field, Q_l is radiation absorption parameter. The term $Q_0(T' - T'_\infty)$ is assumed to be the amount of heat generated or absorbed per unit volume. Q_0 is a constant, which may take on either positive or negative values.

3. Solution of the Problem

In view of (6) the equations (2), (3) and (4) are reduced to the following non-dimensional form

$$\frac{d^2U}{dY^2} + \frac{dU}{dY} - \left(M - \frac{1}{k}\right)U = -GrT - GcC \quad (7)$$

$$\frac{d^2T}{dY^2} + Pr \frac{dT}{dY} - QPrT = -Q_l Pr C - Du Pr \frac{d^2C}{dY^2} \quad (8)$$

$$\frac{d^2C}{dY^2} + Sc \frac{dC}{dY} - KrScC = 0 \quad (9)$$

The corresponding boundary conditions can be written as

$$U = 1, \quad \frac{\partial T}{\partial Y} = -1, \quad \frac{\partial C}{\partial Y} = -1 \quad \text{at } Y = 0 \quad (10)$$

$$u_0 \rightarrow 0, T \rightarrow 0, C = 0 \quad \text{as } Y \rightarrow \infty$$

Where Gr is the thermal Grashof number, Gc is the solutal Grashof number, Pr is the fluid Prandtl number, Sc is the Schmidt number and Kr is the chemical reaction, Q Heat source parameter, Q_l heat absorption.

The study of ordinary differential equations (7), (8) and (9) along with their initial and boundary conditions (10) have been solved by using the method of ordinary linear differential equations with constant coefficients. We get the following analytical solutions for the velocity, temperature and concentration

$$U = D_1 e^{m_4 y} + D_2 e^{m_2 y} + D_3 e^{m_2 y} + D_4 e^{m_2 y} + D_5 e^{m_6 y}$$

$$T = B_1 e^{m_2 y} + B_2 e^{m_2 y} + B_3 e^{m_4 y}$$

$$C = A_1 e^{m_2 y}$$

The computed solution for the velocity is valid at some distance from the slot, even though suction is applied from the slot onward. This is due to the assumption that velocity field is independent of the distance parallel to the plate. The fluids considered in this study are air ($Pr = 0.71$) and water ($Pr = 7.0$).

Skin friction

$$\tau = \left(\frac{\partial U}{\partial y} \right)_{y=0}$$

$$= D_1 m_4 + D_2 m_2 + D_3 m_2 + D_4 m_2 + D_5 m_6$$

Nusselt number

$$Nu = \left(\frac{\partial T}{\partial y} \right)_{y=0} = B_1 m_2 + B_2 m_2 + B_3 m_4$$

Sherwood number

$$Sh = \left(\frac{\partial C}{\partial y} \right)_{y=0} = A_1 m_2$$

Appendix

$$m_2 = -\left(\frac{Sc + \sqrt{Sc^2 + 4KrSc}}{2}\right) m_4 = -\left(\frac{Pr + \sqrt{Pr^2 + 4QPr}}{2}\right) m_2 = -\left(\frac{1 + \sqrt{1 + 4\beta}}{2}\right)$$

$$\alpha = \left(M + \frac{1}{K}\right), A_1 = -\frac{1}{m_2}, B_1 = -\frac{Q_1 A_1 Pr}{m_2^2 + Pr m_2 - QPr}, B_2 = -\frac{Du Pr A_1}{m_2^2 + Pr m_2 - QPr}$$

$$B_3 = -\left(\frac{m_2 B_1 + m_2 B_2 + 1}{m_4}\right), D_1 = -\frac{Gr B_3}{m_4^2 + m_4 - \alpha}, D_2 = -\frac{Gr B_1}{m_4^2 + m_4 - \alpha}$$

$$D_3 = -\frac{Gr B_2}{m_2^2 + m_2 - \alpha} D_4 = -\frac{Gc A_1}{m_2^2 + m_2 - \alpha}, D_5 = (1 - D_1 - D_2 - D_3 - D_4)$$

4. Results and Discussion

Velocity Profiles:

Figures (1) – (10) exhibit the velocity profiles obtained by the numerical simulations for various flow parameters involved in the problem. The simulated parameters are reported in the figure caption. It is evident from figures (1) and (2) that greater cooling of surface, an increase in Gr , and increase in Gc result in an increase in the velocity. It is due to the fact that the increase in the values of Grashof number and modified Grashof number has the tendency to increase the thermal and mass buoyancy effect. The increase is also evident due to the presence of source and chemical reaction parameters. Furthermore the velocity increases rapidly and suddenly falls near the boundary and then approaches the far field boundary condition due to favourable buoyancy force with the increase of both Gr and Gc . It can be seen that the increase in the Prandtl number and Schmidt number leads to a fall in the velocity as shown in figures (1) and (2). The influence of Dufour number on the fluid velocity is illustrated in figures (3). From this figure it is seen that the diffusion thermal effect increases with increasing Dufour number. The velocity profiles for different values of the magnetic field parameter and dimensionless permeability are shown in figure (4). This behaviour is depicted by the decrease in the velocity as permeability decreases and when $K \rightarrow \infty$ (i.e., the porous medium effect is vanishes) the velocity is greater in the flow field. These behaviours are shown in figure (4). Figure (5) shows the velocity profiles for different values of chemical reaction parameter. As the chemical reaction parameter increases, the velocity profile decreases. The effects of magnetic parameter on the velocity field in presence and absence of source and chemical reaction parameter are shown in figure (6). It illustrates that the velocity profile decreases with the increase of magnetic parameter. A little increase in the velocity profile near the boundary layer is marked in figure (7) and (8) with the increase in the Prandtl number the velocity decreases, also convective heat source parameter because the fluid adjacent to the right surface of the plate becomes lighter by hot fluid and rises faster. The boundary layer flows develop adjacent to vertical surface and velocity reaches a maximum in the boundary layer. Figure (9) depicts the velocity profiles for different values of radiation absorption parameter; it is observed that an increasing the radiation absorption parameter the velocity also increases. Figure (10) displays the effects of Schmidt number on the velocity profiles, respectively. As the Schmidt number increases, the velocity decreases. Reductions in the velocity profiles are accompanied by simultaneous reductions in the velocity and concentration boundary layers. These behaviours are evident from figure (10).

Temperature Profiles:

Figures (11) – (16) show the temperature profiles obtained by the numerical simulations for various values of flow parameters. Figure (11) clearly demonstrates that temperature profile of Schmidt number. It can be observed that the amplitude of fluid temperature in presence of heat source decreases; and a similar effect is also observed in figure (12) clearly demonstrates that temperature profile increases due to increase of heat source parameter. The thermal boundary layer thickness increases with an increase in the plate surface convective heat source parameter; but the reverse effect observed in figure (13) for various values of radiation absorption parameter. In figure (14), which the Prandtl number increases the temperature increases it implying higher heat transfer. It is due to that smaller values of Pr means increasing the thermal conductivity, and therefore heat is able to diffuse away from the plate more quickly than higher values of Pr , hence the rate of heat transfer is reduced. The temperatures for different values of chemical reaction parameter shown in figure (15); it is observed that an increasing values of chemical reaction parameter the results is decreases. As the values of Dufour number increase, the fluid temperature also increases shown in figure (16)

Concentration Profile:

Figures (17) and (18) show the concentration profiles obtained by the numerical simulations for various values of non dimensional parameters chemical reaction parameter and Schmidt number. In figure (17) and (18), it is interesting to note that the concentration profiles decrease with the increase of both chemical reaction and Schmidt number. Finally the sheer stress for different values of chemical reaction parameter versus Gr shown in figure (19). It is observed that an increasing values of chemical reaction parameter the results is decreases.

Reference

- Chambre PL, Young JD (1958). On the diffusion of a chemically reactive species in a laminar boundary layer flow, *The Physics of Fluids*,1(1), pp. 48-54.
- D Chenna Kesavaiah and P V Satyanarayana: (2013) MHD and Diffusion Thermo Effects on Flow Accelerated Vertical Plate with Chemical reaction , *Indian Journal of Applied Research*, Volume 3(7), pp. 310-314

Das U N, Deka R K, Soundalgekar V M (1994). Effects of mass transfer on flow past an impulsively started infinite vertical plate with constant heat flux and chemical reaction, *Forschung im Ingenieurwesen*, 60(10), pp. 284-287.

Das U N, Deka R K, Soundalgekar V M (1999): Effects of mass transfer on flow past an impulsively started infinite vertical plate with chemical reaction, *The Bulletin, GUMA*, 5 (1), pp. 13-20.

Gangadhar K, Reddy N B and Kameswaran P K (2012): Similarity solution of hydromagnetic heat and mass transfer over a vertical plate with convective surface boundary condition and chemical reaction, *International Journal of Nonlinear Science*, vol. 3, no. 3, pp. 298–307.

Ibrahim A A (2009): Analytic solution of heat and mass transfer over a permeable stretching plate affected by chemical reaction, internal heating, Dufour – Soret effect and hall effect, *Thermal Science*, 13 (2), pp. 183-97

Manivannan K, Muthucumaraswamy R, Venu T (2009): Radiation and chemical reaction effects on isothermal vertical oscillating plate with variable mass diffusion, *Thermal Science.*, 13 (2), pp. 155-162.

O D Makinde (2010): On MHD heat and mass transfer over a moving vertical plate with a convective surface boundary condition, *Canadian Journal of Chemical Engineering*, vol. 88, no. 6, pp. 983–990.

Olanrewaju P O, Arulogun O T, and K. Adebimpe, (2012): Internal heat generation effect on thermal boundary layer with a convective surface boundary condition,” *American Journal of Fluid Dynamics*, vol. 2, no. 1, pp. 1–4.

Pal D and Chatterjee S (2010): Heat and mass transfer in MHD non-Darcian flow of a micropolar fluid over a stretching sheet embedded in a porous media with non-uniform heat source and thermal radiation, *Commun., Nonlinear Sci., Numer., Simulat.*, 15, pp. 1843-1857

Rahman M M, Eltayeb I A and Rahman S M (2009): Thermo - micropolar fluid flow along a vertical permeable plate with uniform surface heat flux in the presence of heat generation, *Thermal Science*, 13, 1, pp. 23-36

Rout B R, Parida S K, and Panda S (2013): MHD Heat and Mass Transfer of Chemical Reaction Fluid Flow over a Moving Vertical Plate in Presence of Heat Source with Convective Surface Boundary Condition, *International Journal of Chemical Engineering*.

Annexure

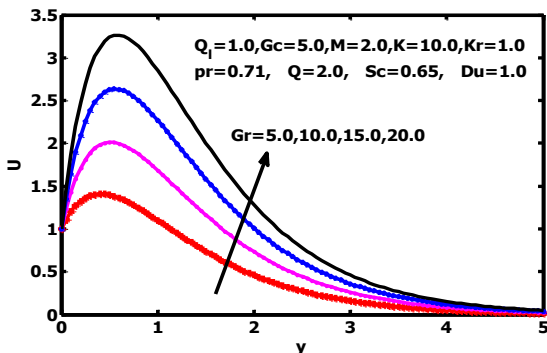


Figure (1): Velocity profiles for different values of Gr

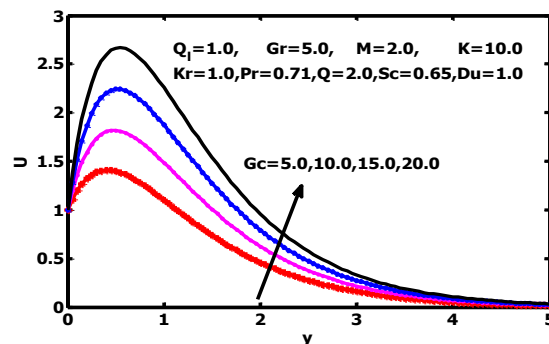


Figure (2): Velocity profiles for different values of Gc

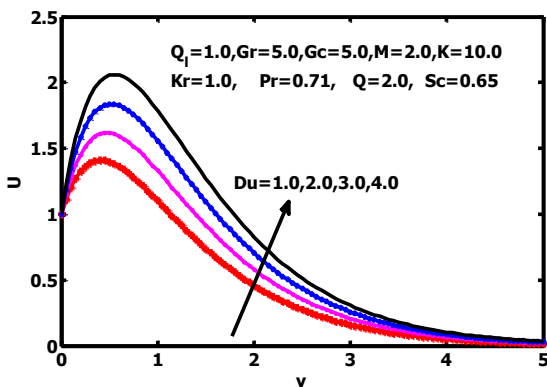


Figure (3): Velocity profiles for different values of Du

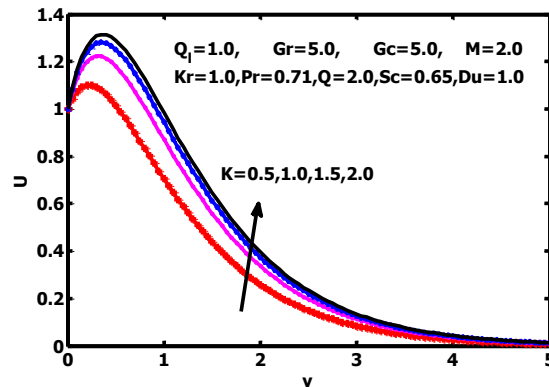


Figure (4): Velocity profiles for different values of K

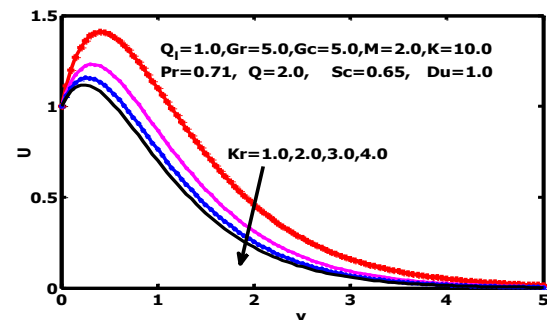


Figure (5): Velocity profiles for different values of Kr

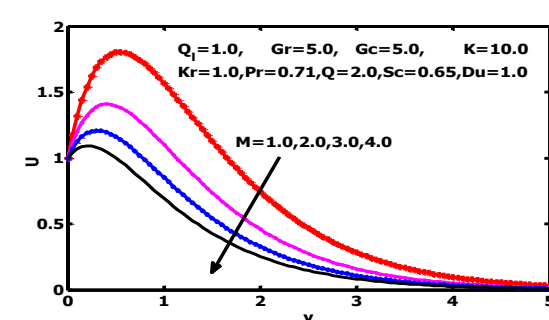


Figure (6): Velocity profiles for different values of M

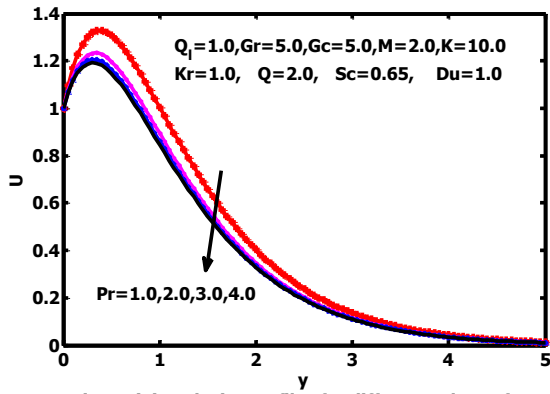


Figure (7): Velocity profiles for different values of Pr

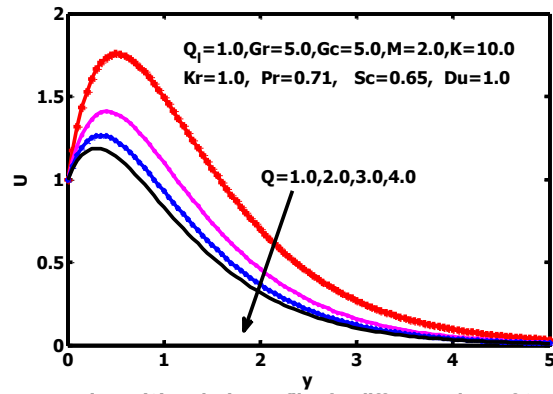


Figure (8): Velocity profiles for different values of Q

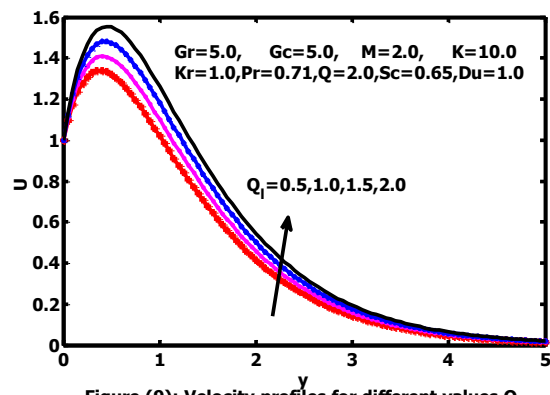


Figure (9): Velocity profiles for different values of Q_1

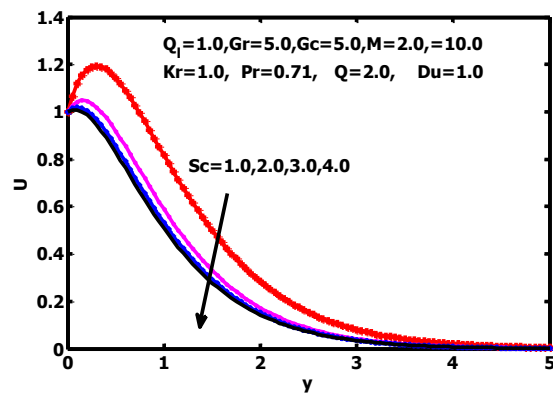


Figure (10): Velocity profiles for different values of Sc

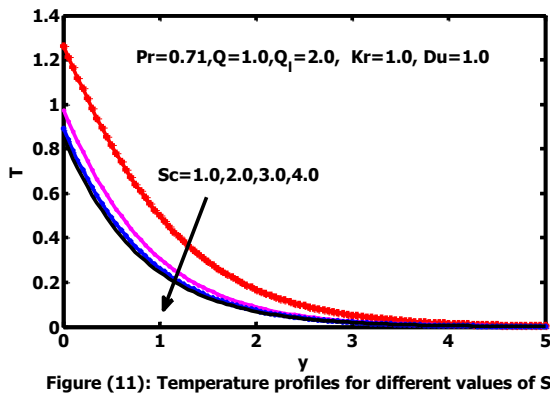


Figure (11): Temperature profiles for different values of Sc

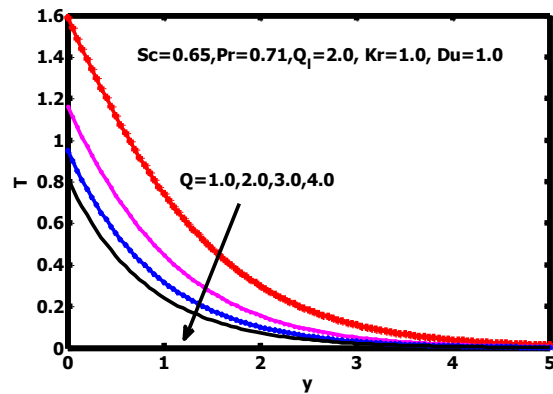


Figure (12): Temperature profiles for different values of Q

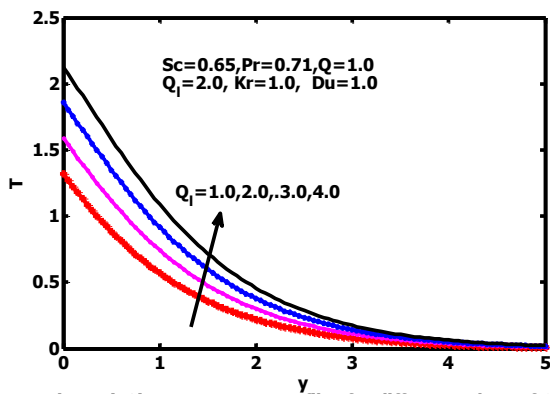


Figure (13): Temperature profiles for different values of Q_1

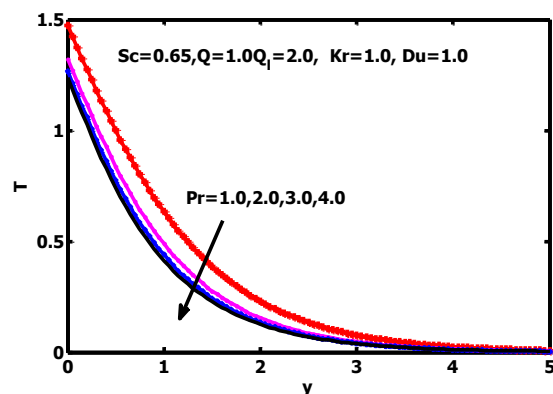


Figure (14): Temperature profiles for different values of Pr

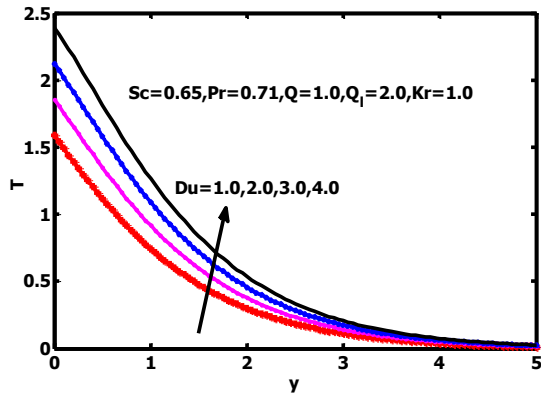


Figure (16): Temperature profiles for different values of Du

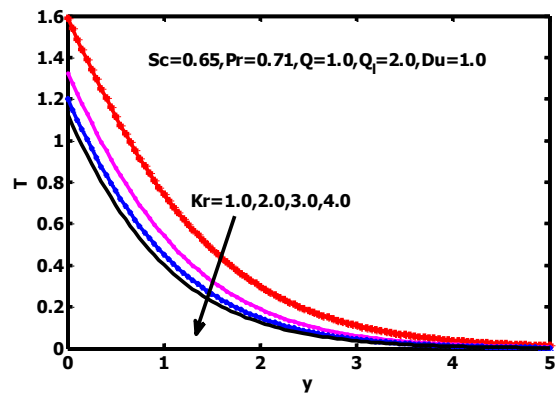


Figure (15): Temperature profiles for different values of Kr

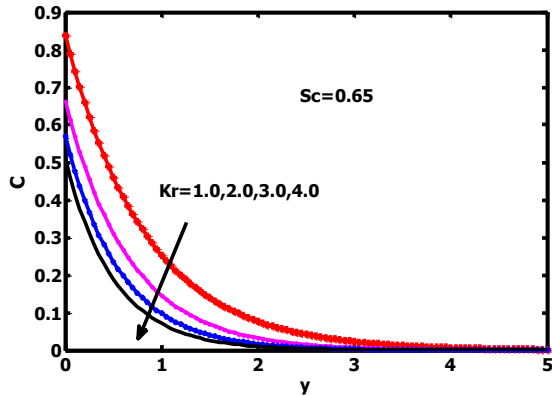


Figure (17): Concentration profiles for different values of Kr

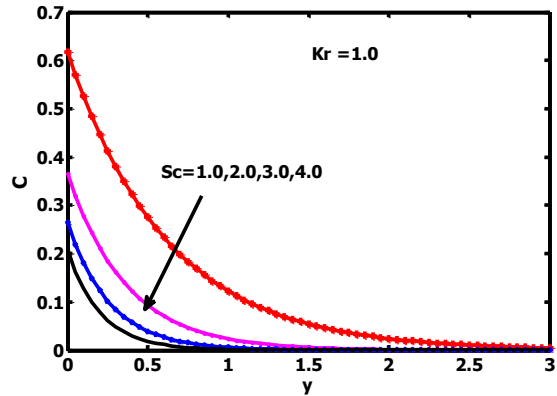


Figure (18): Concentration profiles for different values of Sc

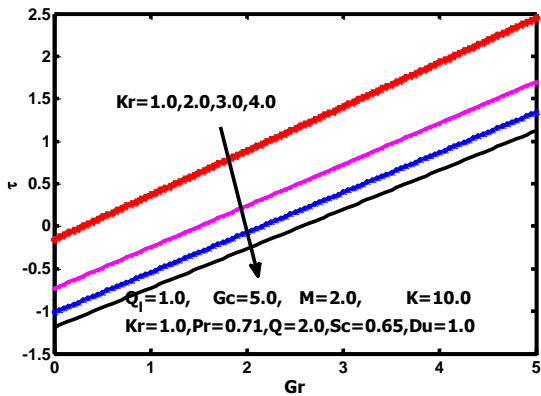


Figure (19): Skin friction for different values of Kr versus Gr